MCB
Journals.ASM.org

Multiple Roles for the Ess1 Prolyl Isomerase in the RNA Polymerase II Transcription Cycle

Zhuo Ma,[a] David Atencio,[a,b] Cassandra Barnes,[b] Holland DeFiglio,[a] and Steven D. Hanes[a,b]

Division of Infectious Disease, Wadsworth Center, New York State Department of Health, Albany, New York, USA,[a] and Department of Biochemistry and Molecular Biology, SUNY—Upstate Medical University, Syracuse, New York, USA[b]

The Ess1 prolyl isomerase in *Saccharomyces cerevisiae* regulates RNA polymerase II (pol II) by isomerizing peptide bonds within the pol II carboxy-terminal domain (CTD) heptapeptide repeat (YSPTSPS). Ess1 preferentially targets the Ser5-Pro6 bond when Ser5 is phosphorylated. Conformational changes in the CTD induced by Ess1 control the recruitment of essential cofactors to the pol II complex and may facilitate the ordered transition between initiation, elongation, termination, and RNA processing. Here, we show that Ess1 associates with the phospho-Ser5 form of polymerase *in vivo*, is present along the entire length of coding genes, and is critical for regulating the phosphorylation of Ser7 within the CTD. In addition, Ess1 represses the initiation of cryptic unstable transcripts (CUTs) and is required for efficient termination of mRNA transcription. Analysis using strains lacking nonsense-mediated decay suggests that as many as half of all yeast genes depend on Ess1 for efficient termination. Finally, we show that Ess1 is required for trimethylation of histone H3 lysine 4 (H3K4). Thus, Ess1 has direct effects on RNA polymerase transcription by controlling cofactor binding via conformationally induced changes in the CTD and indirect effects by influencing chromatin modification.

Peptidyl-prolyl isomerases (PPIases) are enzymes that noncovalently modify target proteins by catalyzing the rotation of the peptide bond preceding proline residues. PPIases catalyze both *cis*→*trans* and *trans*→*cis* peptide bond isomerizations. The resulting changes in protein conformation can have profound functional consequences, such as altering protein-protein interactions, protein stability, or the suitability of a protein as a target for further modifications, e.g., phosphorylation/dephosphorylation (46, 47, 56).

Three classes of PPIases have been identified (5). The parvulin family of PPIases, of which Ess1 (essential 1) protein in *Saccharomyces cerevisiae* is the founding eukaryotic member, is distinct from the well-studied cyclophilin and FK506-binding protein (FKBP) families, which are targets of immunosuppressive drugs. In yeast, Ess1 is required for growth (20), and its human homolog, Pin1, complements yeast *ess1* mutants (32). Pin1 has been linked to a number of signaling pathways in human cells and seems to target a wide variety of proteins for isomerization (33, 70). In contrast, extensive genetic studies have thus far identified only RNA polymerase II (pol II) as the target of Ess1 in yeast (21, 27, 65).

Within the RNA pol II complex, Ess1 targets the carboxy-terminal domain (CTD) of the largest subunit, Rpb1 (38, 65), which is composed of 26 repeats of the heptapeptide $Y_1S_2P_3T_4S_5P_6S_7$ (62). Each repeat contains two potential Ess1 substrate binding sites (S-P), where the serines are known to be phosphorylated (24, 43). *In vitro*, Ess1 binds and isomerizes phosphorylated Ser5-Pro6 (pSer5-Pro6) within the heptad repeat about 5-fold better than pSer2-Pro3 (17). Ess1 stimulates pSer5-Pro6 isomerization within peptide substrates from a rate of less than 1 per minute to >15 per second (17). Genetic data also implicate pSer5-Pro6 as the *in vivo* target (63) where effects on the structure of the CTD, which is highly malleable (37), are likely to be significant.

The CTD is positioned near the exit site for newly synthesized RNA within the RNA polymerase II complex (3) and is thought to help recruit accessory proteins needed for RNA maturation, including cotranscriptional 5′-end capping, transcript elongation, RNA splicing, and termination/3′-end processing (8). Modifications of the CTD, whether covalent (phosphorylation) or noncovalent (isomerization), are therefore likely to be critical for cofactor recruitment during the transcription cycle (7, 14). Indeed, *ess1* conditional mutants show genetic interactions with a number of genes encoding RNA pol II cofactors and exhibit defects in transcription (27, 62, 64). In the best-studied example, *ess1* mutants fail to coordinate the recruitment and release of Nrd1 and Pcf11, which are required for 3′ termination of small noncoding RNAs (ncRNAs) (51). The result is transcription readthrough of snoRNAs and widespread readthrough and stabilization of cryptic unstable transcripts (CUTs) (66), stable unannotated transcripts (SUTs) (41), and other small ncRNAs transcribed by RNA pol II. One likely mechanism is that in the absence of Ess1, the CTD is an unsuitable substrate for the Ser5-Pro6-specific CTD phosphatase, Ssu72 (6, 51, 61, 67). This increases pSer5 levels, resulting in a failure to release Nrd1 and to bind Pcf11 and other factors required for termination and/or 3′-end formation (51, 59). The importance of isomerization of pSer5-Pro6 bonds at different positions along the CTD differs dramatically, with more proximal, N-terminal bonds (near the RNA pol II exit channel) being the target of Ess1 (62).

Here, we investigated three major questions prompted by previous studies. First, does Ess1 influence the recruitment of factors that function during initiation, as suggested by genetic and molecular studies (27, 63)? Second, is Ess1 important for the termi-

Received 23 May 2012 Returned for modification 14 June 2012
Accepted 25 June 2012
Published ahead of print 9 July 2012
Address correspondence to Steven D. Hanes, haness@upstate.edu.
Z.M. and D.A. contributed equally to this work.

doi:10.1128/MCB.00672-12

TABLE 1 *Saccharomyces cerevisiae* strains used in this study

Strain	Genotype	Source
W303-1A	*MAT***a** *ura3-1 trp1-1 leu2-3,112 can1-100 ade2-1 his3-11,15* [*phi*$^+$]	57
W303-1B	*MAT*α *ura3-1 trp1-1 leu2-3,112 can1-100 ade2-1 his3-11,15* [*phi*$^+$]	57
YGD-ts22	*MAT***a** *ura3-1 trp1-1 leu2-3,112 can1-100 ade2-1 his3-11,15 ess1*^{164R}	64
YSB2039	*MAT***a** *ura3-1 trp1-1 leu2-3,112 can1-100 ade2-1 his3-11,15 PCF11-TAP*	S. Buratowski
YSB2040	*MAT***a** *ura3-1 trp1-1 leu2-3,112 can1-100 ade2-1 his3-11,15 PCF11-TAP ess1*^{H164R}	S. Buratowski
YXW137	*MAT***a** *ura3-1 trp1-1 leu2-3,112 can1-100 ade2-1 his3-11,15 ess1*Δ*::HIS3* (pRS315-GAL1-ESS1)	17
YXW138	*MAT***a** *ura3-1 trp1-1 leu2-3,112 can1-100 ade2-1 his3-11,15 ess1*Δ*::HIS3* (pRS315-GAL1-H164R)	17
YJM1	*MAT***a** *ura3-1 trp1-1 leu2-3,112 can1-100 ade2-1 his3-11,15 srb10::TRP1*	63
YJM2	*MAT***a** *ura3-1 trp1-1 leu2-3,112 can1-100 ade2-1 his3-11,15 ess1*^{H164R} *srb10::TRP1*	63
CBW22	*MAT***a** *ura3-1 trp1-1 can1-100 ade2-1 his3-11,15 ess1*Δ*HIS3 srb10::TRP1*	63
46a	*MAT***a** *cup1*Δ *ura3 his3 trp1 lys2 ade2 leu2*	53
46a nrd1-5	*MAT*α *cup1*Δ *ura3 his3 trp1 lys2 ade2 leu2 nrd1-5*	53
YJC1412	*MAT***a** *ade2 can1-100 his3-11,15 leu2-3,112 trp1-1 ura3-1*	12
YJC1098	*MAT***a** *ade2 can1-100 his3-11,15 leu2-3,112 trp1-1 ura3-1 nab3-11*	12
NA67	*MAT*α *ura3-1 leu2-3,112 trp1*Δ *his3-11,15 ade2-1 pcf11-9*	2
BY4741	*MAT***a** *his3*Δ*1 leu2*Δ*0 met15*Δ*0 ura3*Δ*0*	Open Biosystems
Ess1-TAP	*MAT***a** *his3*Δ*1 leu2*Δ*0 met15*Δ*0 ura3*Δ*0 ESS1-TAP::HIS3*	Open Biosystems
BY4742	*MAT*α *his3*Δ*1 leu2*Δ*0 lys2*Δ*0 ura3*Δ*0*	Open Biosystems
YHD154	*MAT***a** *ura3-1 leu2-3,112 trp1-1 can1-100 ade2-1 his3-11,15* [*phi*$^+$] *BYE1-TAP* tag::*HIS3MX6*	This study
YHD152	*MAT***a** *ura3-1 leu2-3,112 trp1-1 can1-100 ade2-1 his3-11,15* [*phi*$^+$] *BYE1-TAP* tag::*HIS3MX6 ess1*^{H164R}	This study
YHD139	*MAT***a** *ura3-1 leu2-3,112 trp1-1 can1-100 ade2-1 his3-11,15* [*phi*$^+$] *PAF1-TAP* tag::*HIS3MX6*	This study
YHD129	*MAT***a** *ura3-1 leu2-3,112 trp1-1 can1-100 ade2-1 his3-11,15* [*phi*$^+$] *PAF1-TAP* tag::*HIS3MX6 ess1*^{H164R}	This study
YHD146	*MAT***a** *ura3-1 leu2-3,112 trp1-1 can1-100 ade2-1 his3-11,15* [*phi*$^+$] *SPT4-TAP* tag::*HIS3MX6*	This study
YHD150	*MAT***a** *ura3-1 leu2-3,112 trp1-1 can1-100 ade2-1 his3-11,15* [*phi*$^+$] *SPT4-TAP* tag::*HIS3MX6 ess1*^{H164R}	This study
YHD136	*MAT***a** *ura3-1 leu2-3,112 trp1-1 can1-100 ade2-1 his3-11,15* [*phi*$^+$] *SEN1-TAP* tag::*HIS3MX6*	This study
YHD125	*MAT***a** *ura3-1 leu2-3,112 trp1-1 can1-100 ade2-1 his3-11,15* [*phi*$^+$] *SEN1-TAP* tag::*HIS3MX6 ess1*^{H164R}	This study
YHD132	*MAT***a** *ura3-1 leu2-3,112 trp1-1 can1-100 ade2-1 his3-11,15* [*phi*$^+$] *CEG1-MYC* tag::*TRP1* (from *Kluyveromyces lactis*)	This study
YHD119	*MAT***a** *ura3-1 leu2-3,112 trp1-1 can1-100 ade2-1 his3-11,15* [*phi*$^+$] *ess1*^{H164R} *CEG1-MYC* tag::*TRP1* (from *K. lactis*)	This study
YDA500	*MAT*α *his3*Δ*1 leu2*Δ*0 lys2*Δ*0 ura3*Δ*0 ESS1::natMX4*	This study
YDA502	*MAT*α *his3*Δ*1 leu2*Δ*0 lys2*Δ*0 ura3*Δ*0 ess1*^{H164R}*::natMX4*	This study
YDA511	*MAT***a** *his3*Δ*1 leu2*Δ*0 met15*Δ*0 ura3*Δ*0 set1*Δ*::kanMX4*	This study
YDA512	*MAT*α *his3*Δ*1 leu2*Δ*0 lys2*Δ*0 ura3*Δ*0 ESS1::natMX4 set1*Δ*::kanMX4*	This study
YDA516	*MAT*α *his3*Δ*1 leu2*Δ*0 lys2*Δ*0 ura3*Δ*0 ess1*^{H164R}*::natMX4 set1*Δ*::kanMX4*	This study
YDA587	*MAT*α *his3*Δ*1 leu2*Δ*0 lys2*Δ*0 ura3*Δ*0 ess1*^{H164R}*::natMX4 jhd2*Δ*::kanMX4*	This study
YDA554	*MAT*α *his3*Δ*1 leu2*Δ*0 lys2*Δ*0 ura3*Δ*0 ESS1::natMX4 nam7*Δ*::kanMX4*	This study
YDA556	*MAT*α *his3*Δ*1 leu2*Δ*0 lys2*Δ*0 ura3*Δ*0 ess1*^{H164R}*::natMX4 nam7*Δ*::kanMX4*	This study
YDA558	*MAT*α *his3*Δ*1 leu2*Δ*0 lys2*Δ*0 ura3*Δ*0 ESS1::natMX4 rrp6*Δ*::kanMX4*	This study
YDA560	*MAT*α *his3*Δ*1 leu2*Δ*0 lys2*Δ*0 ura3*Δ*0 ess1*^{H164R}*::natMX4 rrp6*Δ*::kanMX4*	This study
YDA565	*MAT*α *his3*Δ*1 leu2*Δ*0 lys2*Δ*0 ura3*Δ*0 ESS1::natMX4 xrn1*Δ*::kanMX4*	This study
YDA568	*MAT*α *his3*Δ*1 leu2*Δ*0 lys2*Δ*0 ura3*Δ*0 ess1*^{H164R}*::natMX4 xrn1*Δ*::kanMX4*	This study
Y10158	*MAT***a** *his3*Δ*1 leu2*Δ*0 met15*Δ*0 ura3*Δ*0 lcb1-4::kanMX4*	31
Y11354	*MAT***a** *his3*Δ*1 leu2*Δ*0 met15*Δ*0 ura3*Δ*0 srm1-ts::kanMX4*	31
Y07833	*MAT***a** *his3*Δ*1 leu2*Δ*0 met15*Δ*0 ura3*Δ*0 kar2-159::kanMX4*	31
Y10345	*MAT***a** *his3*Δ*1 leu2*Δ*0 met15*Δ*0 ura3*Δ*0 hts1-1::kanMX4*	31
Y04855	*MAT***a** *his3*Δ*1 leu2*Δ*0 met15*Δ*0 ura3*Δ*0 pri2-1::kanMX4*	31
Y07794	*MAT***a** *his3*Δ*1 leu2*Δ*0 met15*Δ*0 ura3*Δ*0 bos1-1::kanMX4*	31

nation of mRNAs, as inferred genetically (21, 64)? And third, are the actions of chromatin modifiers, which may be sensitive to the phosphorylation state of the CTD (9, 52), also influenced by Ess1 (4)? These and other questions regarding the role of Ess1 during the transcription cycle are addressed. The results indicate that Ess1 functions in multiple steps of transcription; it inhibits ncRNA initiation, stimulates mRNA termination, and controls the phosphorylation state of CTD Ser7 (as well as Ser5). Finally, Ess1 is required for proper chromatin modification, specifically, the methylation of histone H3 lysine 4 (H3K4). The results support the model that Ess1 helps coordinate RNA pol II cofactor recruitment and function.

MATERIALS AND METHODS

Yeast strains, plasmids, oligonucleotides, and growth conditions. Yeast strains are listed in Table 1. Strains YDA50 0 and YDA502 were generated using a sewing PCR strategy to insert a *natMX* cassette adjacent to wild-type *ESS1* or *ess1*^{H164R} in strain BY4742. Transformants were selected on clonNAT (nourseothricin; Werner BioAgents, Jena, Germany), and the insertions confirmed by PCR and DNA sequencing. Strain YDA511 (*set1*Δ) was made in the BY4741 background by replacing *SET1* with *kanMX*, using G418 selection (Invitrogen). Plasmid p4339 (source of *natMX*) was a gift of Ian Willis, pUG6 (source of *kanMX*) was a gift of Joan Curcio, and PrADH1-HA-SET1 (pMP803) was a gift of Bernard Dichtl (19). Oligonucleotides were synthesized by Integrated DNA Technologies, and their sequences are available upon request. Yeast strains were

cultured using standard conditions and media (49). Double mutants were generated by crosses and tetrad dissection using deletion strains from the EUROSCARF collection.

Coimmunoprecipitation (co-IP). Wild-type yeast (W303-1A) was grown in 30 ml yeast extract-peptone-dextrose (YEPD) medium to an optical density at 600 nm (OD_{600}) of 0.6, and cells were pelleted, washed, and resuspended in FA lysis buffer (50 mM HEPES-KOH, pH 7.5, 140 mM NaCl, 1 mM EDTA, pH 8, 1% Triton X-100, 0.1% sodium deoxycholate with 1× protease, and phosphatase inhibitors) and broken with an equal volume of glass beads using a cell disruptor at 4°C. The extracts were clarified by microcentrifugation at 14,000 rpm. The protein concentration was determined using a Bio-Rad protein assay. About 2 mg of total protein lysate was incubated with 5 μl affinity-purified anti-Ess1 antibody overnight at 4°C. Thirty microliters of protein A-agarose bead slurry was added for 2 h, followed by 2 washes with low-salt (140 mM NaCl) and high-salt (250 mM NaCl) FA lysis buffers. Protein A-agarose beads were resuspended in 30 μl FA lysis buffer and 30 μl 2× sample buffer (62.5 mM Tris-HCl, pH 6.8, 25% glycerol, 2% SDS, 0.01% bromophenol blue, 5% beta-mercaptoethanol), boiled for 10 min, and clarified by centrifugation. Supernatants were loaded on 8% SDS-PAGE gels for Western blot detection of hypophospho-CTD, pSer5, and pSer2, as well as Ess1, with antibodies described below.

Western analysis. Western analysis was carried out as described previously (51). The primary antibodies were H14 (pSer5) and 8WG16 (hypophosphorylated CTD) from Covance, H5 (pSer2) from Bethyl, 4E12 (pSer7) (11), anti-H3K4me3 (trimethylated H3K4) from Upstate, anti-H3K36me3 and anti-H3 from Abcam, and anti-Ess1 (65). Antitubulin antibody (Abcam) was used for loading controls. Secondary monoclonal antibodies (MAbs; anti-mouse, anti-rat, or anti-rabbit immunoglobulin, IgG, or anti-mouse IgM) conjugated to horseradish peroxidase (Amersham) were used as appropriate.

ChIP. Chromatin immunoprecipitation (ChIP) was performed as described previously (51). The antibodies used were as follows: anti-Ess1 (65), anti-Rpb3 (1:100 dilution; Neoclone), anti-pSer2 (1:100 dilution), anti-pSer5 (1:100 dilution), anti-TATA binding protein (1:100 dilution; Santa Cruz), anti-TFIIB (1:100 dilution; a gift of Anthony Weil), anti-Ssu72 (1:100 dilution; a gift of Michael Hampsey), anti-TFIIS (1:100 dilution; a gift of Caroline Kane), anti-Nrd1 (1:100 dilution; a gift of D. Brow), anti-H3K4me3 (1 μl; Upstate), anti-H3K36me3 (1 μl; Abcam), and anti-H3 (1 μl; Abcam) antibodies. Tandem affinity purification (TAP)-tagged proteins (Pcf11, Sen1, Paf1, Spt4, and Bye1) were immunoprecipitated using anti-protein A and then with protein A-agarose (Santa Cruz). Myc-tagged protein (Ceg1) was precipitated using anti-Myc antibody (Santa Cruz) and protein A-agarose. For each antibody, the immunoprecipitated DNA fragments from at least three biological replicates were isolated. The relative proportion was then analyzed by quantitative real-time PCR (qRT-PCR). For normalization across a set of samples, quantitative real-time PCR values (normalized to inputs and a chromosome V control, except that for H3K4me3, a tRNA gene was used for internal control) were summed for each experiment and the sums set to the same arbitrary value. The normalized values thus obtained for each ChIP sample were then used to obtain averages and standard deviations (71). For the experiment whose results are shown in Fig. 4, ChIP samples were analyzed using standard PCR (26 cycles) and products resolved by gel electrophoresis. Ethidium bromide-stained gel scans were quantitated using ImageJ software. Representative results from one of three replicates (for *PYK1*, *PTC1*, and *ARD1*) or two replicates (for *BUD3*) are shown.

RNA isolation, cDNA synthesis, qRT-PCR, and Northern analysis. Cells were grown at 30°C to an OD_{600} of 0.5 to 0.8. For Northern analysis, cells were shifted to 37°C for 2 h. RNA was purified using hot phenol as described previously (48). The RNA was treated with DNase (Turbo DNA-free DNase; Ambion) and quantitated spectrophotometrically. An aliquot was used for qRT-PCR (described below) to test the efficacy of the DNase treatment. cDNA synthesis was carried out in a 10-μl reaction mixture containing 1 μg of RNA, random hexamers at 3.75 μM or gene-specific primers at 500 nM, and deoxynucleoside triphosphates (dNTPs) at 500 μM. This was incubated at 65°C for 10 min to denature the RNA. Two units of RNase inhibitor (USB), 1 U Moloney murine leukemia virus (M-MLV) reverse transcriptase (USB),10× buffer (supplied), and water were added to bring the reaction mixture to 1×, followed by incubation at 44°C for 1 h. Amounts of 0.5 μl of this cDNA and 1 μl of a primer mixture at 10 μM each were added to 6.25 μl of HotStart-IT SYBR green qPCR master mix (USB) and 4.75 μl H_2O. qRT-PCR was carried out in an Eppendorf Realplex Mastercycler Epgradient S as follows: 95°C for 2 min, followed by 40 cycles of 95°C 15 s, 60°C 15 s, and 68°C for 20 s. All PCR primers were tested for efficiency on DNA templates using standard reaction mixtures, and the products examined on ethidium bromide-stained gels. The comparative C_T (cycle threshold) method (Applied Biosystems), in which the amount of target gene amplification is normalized to the amplification of an NADPH internal control, was used for quantitation. The relative (fold) enrichment is calculated as follows: $2^{-\Delta\Delta CT} = 2^{[\Delta CT\,(\text{control}) - \Delta CT\,(\text{sample})]}$, where $\Delta C_T = C_T(\text{sample}) - C_T(\text{control})$. Error bars in figures show standard deviations from the mean log values of at least three biological replicates. The internal control was the *SNR6* gene (a pol III product), and all values were normalized to the transcript levels in the upstream coding region as follows: [(intergenic region/SNR6)/(upstream control/SNR6)]mutant/[(intergenic region/SNR6)/(upstream control/SNR6)]wild type. Northern analysis was carried out by standard methods, using formaldehyde gel electrophoresis, GeneScreen+ membranes (Perkin-Elmer), and ^{32}P-labeled probes ([α-^{32}P]dATP, 3,000 Ci/mmol; Perkin-Elmer) generated by random priming (Sequenase; USB-Affymetrix) of glass powder-and-gel-purified PCR-generated gene fragments.

RESULTS

Ess1 targets pSer5-CTD and controls Ser7 phosphorylation levels. To test whether Ess1 associates with the pSer5 form of RNA pol II *in vivo*, we performed coimmunoprecipitation (co-IP) experiments. Rabbit anti-Ess1 antibodies were used against yeast whole-cell extracts, and the precipitates analyzed by Western blotting with CTD phospho-specific antibodies. The results indicate that Ess1 preferentially associates with the pSer5 form or the pSer2-pSer5 doubly phosphorylated form, which is also recognized by the H14 MAb (11), over the pSer2 alone or hypophosphorylated forms of pol II (Fig. 1A). Thus, the specificity of Ess1 *in vivo* appears to be similar to that defined *in vitro* and by genetic inference (17, 63).

We and others showed that the levels of pSer5 become elevated in *ess1* mutant cells, whereas the levels of pSer2 remain unchanged (6, 27, 51). This is probably due to loss of Ess1-directed prolyl bond isomerization at pSer5-Pro6 and consequent reduction of the affinity of the Ssu72 phosphatase, which targets pSer5 (61). Ser7 phosphorylation in the CTD seems to be linked to that of Ser5 (15, 26, 36, 58). We therefore examined whether the levels of Ser7 phosphorylation are affected in *ess1* mutant cells. Using two different mutants (*ess1*^{H164R} and *ess1*Δ *srb10*Δ), Western blotting of whole-cell extracts with pSer7-specific antibodies showed that pSer7 levels were indeed elevated (Fig. 1B), mirroring those of pSer5 (51). Note that pSer7 is followed not by a proline residue in the CTD (Y-S-P-T-S-P-S)$_n$ but, rather, by a tyrosine. Therefore, the effect of Ess1 on Ser7 phosphorylation is likely to occur by an indirect mechanism, perhaps involving a processive coupling of dephosphorylation by Ssu72 that initiates at pSer5-Pro6. Genome-wide analysis has also implicated Ess1 in control of pSer7 levels (6). One potential caveat to these experiments is the possibility that loss of Ess1 activity alters the isomeric state of the CTD in such a way as to increase recognition by the monoclonal anti-

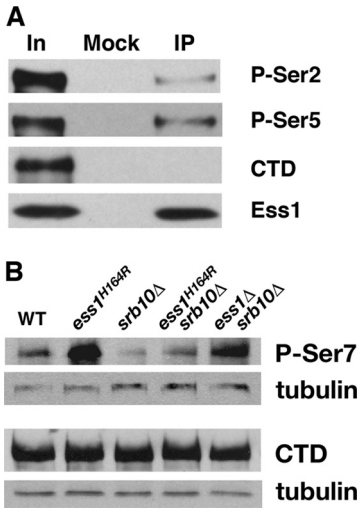

FIG 1 Ess1 preferentially associates with pSer5 CTD *in vivo* and promotes dephosphorylation of pSer7 CTD. (A) Wild-type (WT) cells were subjected to immunoprecipitation (IP) with anti-Ess1 polyclonal antibodies, followed by Western analysis with monoclonal antibodies H5 (P-Ser2), H14 (P-Ser5), and 8WG16 (hypophosphorylated CTD). Sample inputs (In) are indicated. Note that the H14 antibody actually recognizes doubly phosphorylated pSer2/pSer5 (11). (B) Western analysis of protein (10 μg) from whole-cell extracts of the indicated strains grown at 30°C. The 4E12 monoclonal antibody was used to detect levels of pSer7 CTD, and the 8WG16 monoclonal antibody (hypophosphorylated CTD) as a control for overall levels of RNA pol II CTD. Antitubulin antibodies were used for detection of the loading control. Note that *ESS1* is an essential gene but can be suppressed by deletion of *SRB10* (62).

bodies used for detecting the phosphorylated form of Ser7. We do not favor this explanation, however, as the increase in Ser7 phosphorylation appears to be greater than stoichiometric, suggesting a catalytic effect, more consistent with a loss of Ess1's known stimulation of protein phosphatase activity (61).

Ess1 represses initiation of small noncoding RNAs. A genome-wide tiling microarray analysis of *ess1* mutants led to the discovery of defects in Nrd1-dependent transcription termination of small noncoding RNAs (51). A large number of CUTs were also identified in *ess1* mutants. To study their production further, we used chromatin immunoprecipitation (ChIP) to compare the pol II CTD phosphorylation profiles and localization of various transcription cofactors across representative loci in wild-type and *ess1* mutant cells.

Three loci were chosen for study. First, we chose the *TEF2-MUD2* locus, where we found a prominent previously annotated CUT (51, 66) to be upregulated in *ess1* mutant cells, as well as the *RNQ1-FUS1* locus that contains a putative CUT. Second, we examined the *SRG1-SER3* locus, where *SRG1* is a SUT-like noncoding RNA that represses the expression of *SER3* in response to serine levels via a mechanism of transcriptional interference (35). Finally, the *PYK1* gene served as a control for a midsized protein-coding gene (~1.5 kb) that contained no obvious CUTs in *ess1* mutants (51).

In the first set of experiments, we carried out ChIP across these loci using pSer2-specific (H5) or pSer5-specific (H14) antibodies. Antibodies to the Rpb3 subunit of RNA pol II were used as a control for the total amount of pol II complex present. The results revealed an increase in the total amount of pol II complex recruited to the position of the NBR024W CUT, the putative *RNQ1-FUS1* intergenic CUT, and *SRG1* in the *ess1* mutant (Fig. 2A to C). Most of the increases are due to enrichment of the pSer5 form of the pol II CTD, consistent with elevated pSer5 levels at the 5′ ends of actively transcribed genes. The control gene, *PYK1*, did not show either any substantive changes in pSer5 or pSer2 phosphorylation (Fig. 2D) or changes in expression in *ess1* mutant cells (51).

In the second set of experiments, we examined recruitment to three loci of selected cofactors important for initiation, elongation, and termination of transcription. Consistent with the strong induction of the NBR024W CUT, the recruitment of TATA-binding protein (TBP), the TFIIB initiation factor, and capping enzyme Ceg1 all increased (Fig. 3A). Similar results were observed at the *SRG1* locus. For both loci, the majority of the increase in recruitment occurred at a position encompassing the beginning of the CUT transcripts. In contrast, there was no enhancement of initiation factors on the *PYK1* gene in *ess1* mutant cells. These results suggest that in *ess1* mutants, increased production of small noncoding RNAs is due, at least in part, to increased transcription initiation. Thus, one role of Ess1 in wild-type cells is to repress CUT/small ncRNA initiation.

Similar experiments were performed to examine recruitment of elongation (Fig. 3B). For elongation factors TFIIS and Paf1, we found no alteration in recruitment, and for Spt4, the changes did not appear significant (Fig. 3B). In contrast, we observed a strong increase in recruitment of Bye1 in *ess1* mutants (Fig. 3B). The latter is not entirely surprising given that Bye1 was discovered as a high-copy-number suppressor of Ess1, and it is possible that in the absence of Ess1, high levels of Bye1 play a substitute role in controlling elongation (63). Given that TFIIS, Paf1, and Spt4 function to promote elongation, whereas Bye1 acts to inhibit elongation (64), it seems unlikely that stimulation of elongation is a decisive event in CUT/small ncRNA induction in *ess1* mutants.

Finally, we examined termination factor recruitment. We chose two factors important for small ncRNA termination, Nrd1 and Sen1, and two factors that work universally in termination, Pcf11 (which binds the CTD and nascent RNA) and Ssu72, the Ser5 phosphatase that is required for termination and 3′-end processing. No change was observed for Ssu72 or Sen1 recruitment on any of the loci examined (Fig. 4). In the case of Ssu72, this enzyme might bind normally but not be able to dephosphorylate the CTD because it is not in the preferred isomerization state (*cis*) (61). In contrast, in the *ess1* mutant, recruitment of Nrd1 is increased and Pcf11 is decreased on the NBR024W, *SRG1*, and *RNQ1-FUS1* loci (Fig. 4), similar to earlier studies on snoRNA termination sites (51). This aberrant recruitment pattern might lead to transcription readthrough, as previously observed (51). In summary, the CTD phosphorylation and ChIP data are consistent with the idea that increased initiation and aberrant termination contribute to CUT and small ncRNA overexpression/stabilization in *ess1* mutants. Ess1's normal function, therefore, is to repress aberrant initiation of CUTs/SUTs, as well as to promote their proper termination.

Ess1 is localized along mRNA coding genes. Our tiling array of *ess1* mutants revealed readthrough of mRNA genes only in rare instances (51). We wondered whether this was because Ess1 does not bind to RNA pol II engaged on longer transcription units and therefore, plays no role in termination of mRNAs. To address this question, we carried out ChIP to localize Ess1 protein across mRNA genes of various lengths. The genes analyzed were *PYK1* (1.5 kb), *PTC1* (0.8 kb), *BUD3* (6.4 kb), and *ARD1* (0.7 kb) (Fig.

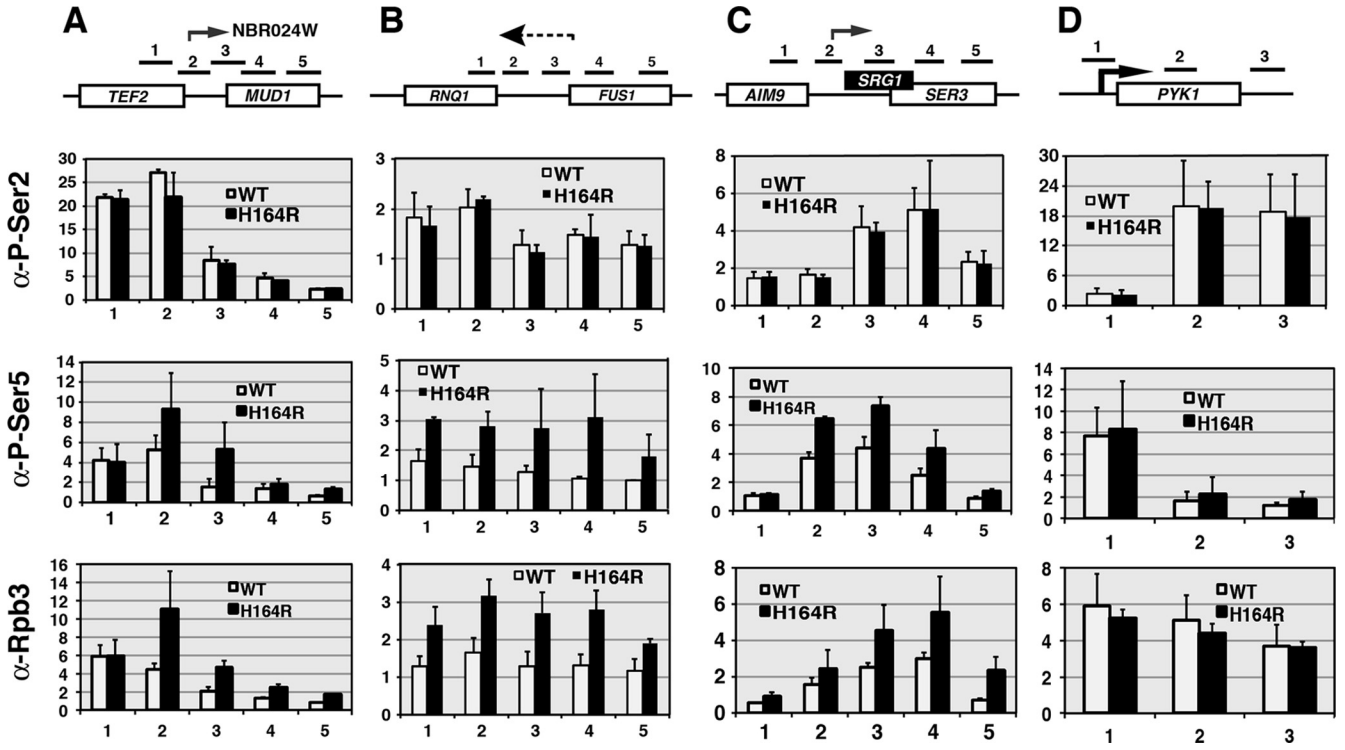

FIG 2 Ess1 mutants show increased recruitment to ncRNA loci of the initiation form (pSer5) of RNA pol II. Wild-type and *ess1*^{H164R} mutant cells were grown to mid-logarithmic phase at 30°C. Chromatin immunoprecipitation was used to monitor recruitment of total RNA pol II complex (α-Rpb3) and the pSer2 or pSer5 forms of Rpb1. (A to C) Results of ChIP across three intergenic regions containing known CUTs (*NBR024W* and *SRG1*) or a suspected CUT (between *RNQ1* and *FUS1*). Increased recruitment of the pSer5 but not the pSer2 form of pol II is detected in all three. (D) Results of control ChIP across the PYK1-coding gene locus. No increase in recruitment of either form of pol II is detected. Fold changes are relative to the results for a chromosome V control. Numbered horizontal bars represent approximate locations of qRT-PCR products (also in Fig. 3, 4, and 9). Error bars show standard deviations of three biological replicates.

5A). Quantitation of these results indicates that Ess1 was present at 5′, middle, and 3′ locations, although the amount of Ess1 varied between loci (Fig. 5B). As expected, a control ChIP shows localization of TBP to the 5′ end of the *PYK1* gene. These results suggest that Ess1 associates with RNA pol II across the entire length of protein-coding genes. Thus, our failure to detect an effect on mRNA termination was not due to the lack of Ess1 on protein-coding genes.

Ess1 is required for efficient mRNA termination. We next considered the possibility that Ess1 might be important for mRNA gene termination but, in *ess1* mutants, readthrough transcripts were degraded by an RNA surveillance mechanism (1). This would have precluded their detection using a tiling microarray approach (51). First, we carried out genetic interaction tests to determine whether nonsense-mediated decay (NMD) was involved (39). We generated double-mutant cells that were defective for both *ess1* and genes required for NMD, including *UPF1* (also known as *NAM7*), which encodes an RNA helicase that plays a key role in nonsense recognition and targeting of aberrant RNAs (29). In addition, we made double mutants with *XRN1* (cytoplasmic 5′→3′ exonuclease) and *RRP6* (nuclear 3′→5′ exonuclease), which encode P-body and exosome components required for degrading aberrant mRNAs. The prediction is that the severity of the growth defect of an *ess1*^{ts} conditional mutant would be enhanced in a background that failed to degrade readthrough transcripts. This is exactly what we observed (Fig. 6), with severe growth defects in the double mutants apparent even at 30°C, which is normally permissive for the growth of *ess1*^{H164R} cells.

To determine whether loss of NMD stabilized mRNA readthrough transcripts in *ess1* mutants, we looked directly for readthrough products using reverse transcription-PCR. To simplify the analysis, we examined loci that met the following criteria: (i) mRNA genes that did not show obvious readthrough in our prior tiling array analysis (51), (ii) genes that were oriented in the same direction so as to avoid potential transcriptional interference by converging polymerases, and (iii) loci that lacked obvious CUTs in *ess1* mutants (based on prior tiling array data).

The initial experiments were done using random hexamers as primers for reverse transcription, followed by PCR to detect intergenic transcripts. Nearly all 14 loci examined displayed intergenic transcription in *ess1* mutants. Representative data for three loci are shown (Fig. 7A) and reveal strong intergenic transcription in *ess1* mutants for two of the three loci (*TAE1-RGD1* and *SMK1-SEC8*). For the third locus (*HMG2-LEU3*), only a small increase in transcript levels relative to the levels in wild-type cells was detected. Importantly, for *TAE1-RGD1*, the intergenic transcripts are dramatically increased in the NMD-deficient background (*ess1*^{H164R} *upf1*Δ) (Fig. 7A), suggesting that they are normally degraded by NMD. The intergenic transcription could result from mRNA readthrough but could also be due to CUTs or other small ncRNAs templated from either DNA strand (see schematic).

To help distinguish CUTs from readthrough transcripts, we used gene-specific (and strand-specific) primers for reverse transcription of RNA that would only allow the detection of forward transcripts (Fig. 7B, schematic). We also used an additional primer set at each locus that allowed the detection of longer fusion

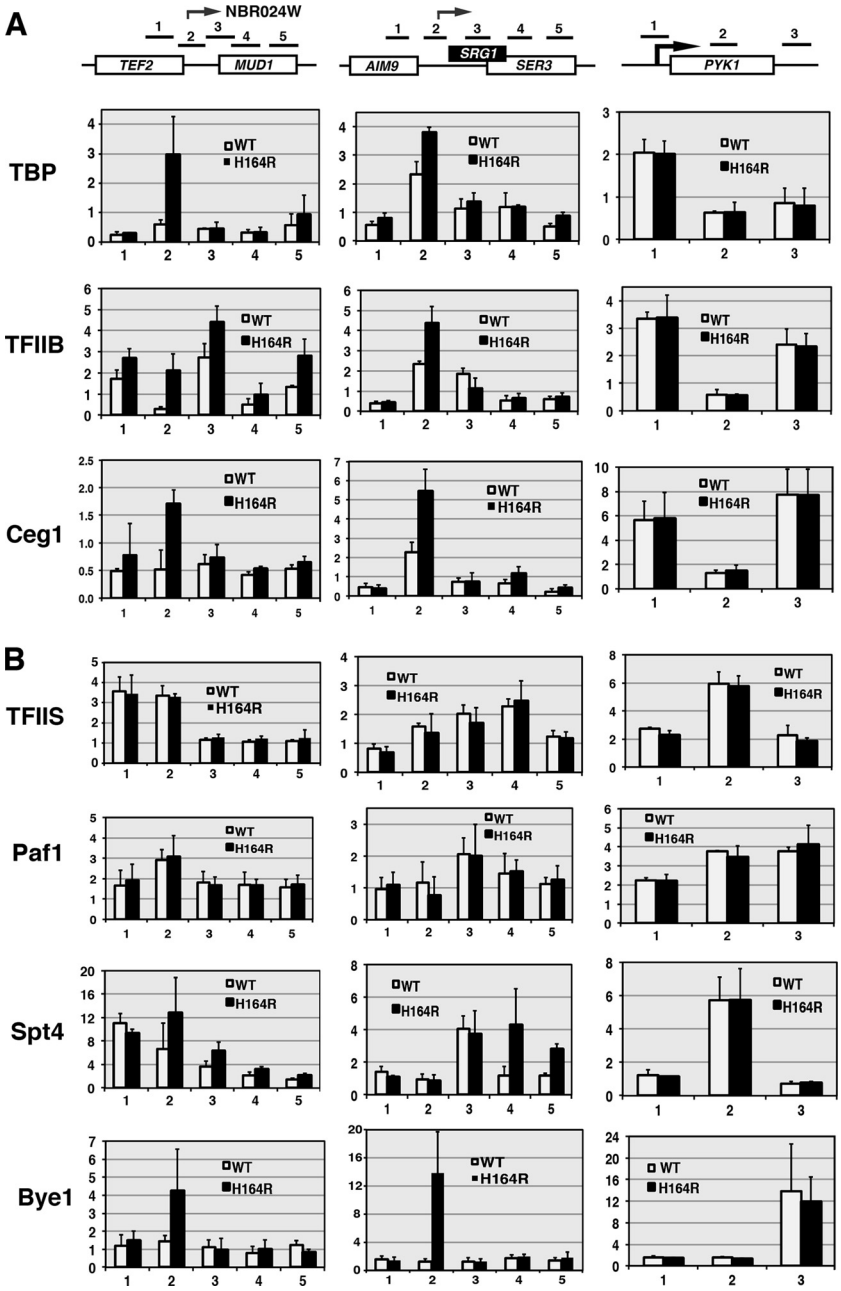

FIG 3 Ess1 mutants show increased recruitment of the initiation factors but not general elongation factors to ncRNA loci. (A) Results of ChIP to detect recruitment of Ceg1 (capping enzyme), and initiation factors TBP and TFIIB to ncRNA loci in *ess1*^{H164R} mutant cells. Increases are detected across intergenic regions of *TEF2-MUD1* and *SRG1* but not on the coding gene *PYK1*. (B) ChIP to monitor recruitment of elongation factors. No significant changes are detected in *ess1*^{H164R} cells for TFIIS and Paf1. Spt4 shows a modest increase on *SRG1*. A larger increase in recruitment of the *ess1*-specific suppressor Bye1 (bypass of Ess1) is detected on ncRNA loci in *ess1*^{H164R} cells.

transcripts (potential readthroughs) composed of both coding and downstream intergenic sequences. As shown in Fig. 7B, both short intergenic (primer set 1) and long fusion transcripts (primer set 2) are detected at the *TAE1-RGD1* locus, and both are stabilized in the NMD-deficient background. In contrast, at the *SMK1-SEC8* locus, only the short intergenic transcripts and not the long fusion transcripts are detected, suggesting the presence of a forward-oriented CUT.

The gel data (Fig. 7A and B) illustrate key points, but are only qualitative. We also took a quantitative approach on more than a dozen individual loci using reverse transcription–real-time PCR (Table 2). The results are expressed relative to the results for the wild type and as a ratio of the amount of intergenic transcript relative to the amount of upstream mRNA to normalize for any changes that might occur in the transcription of the gene in mutant backgrounds. For the 14 loci examined, changes in upstream gene expression (data not shown) were minor if any compared with changes in the levels of intergenic transcripts (Table 2). Each

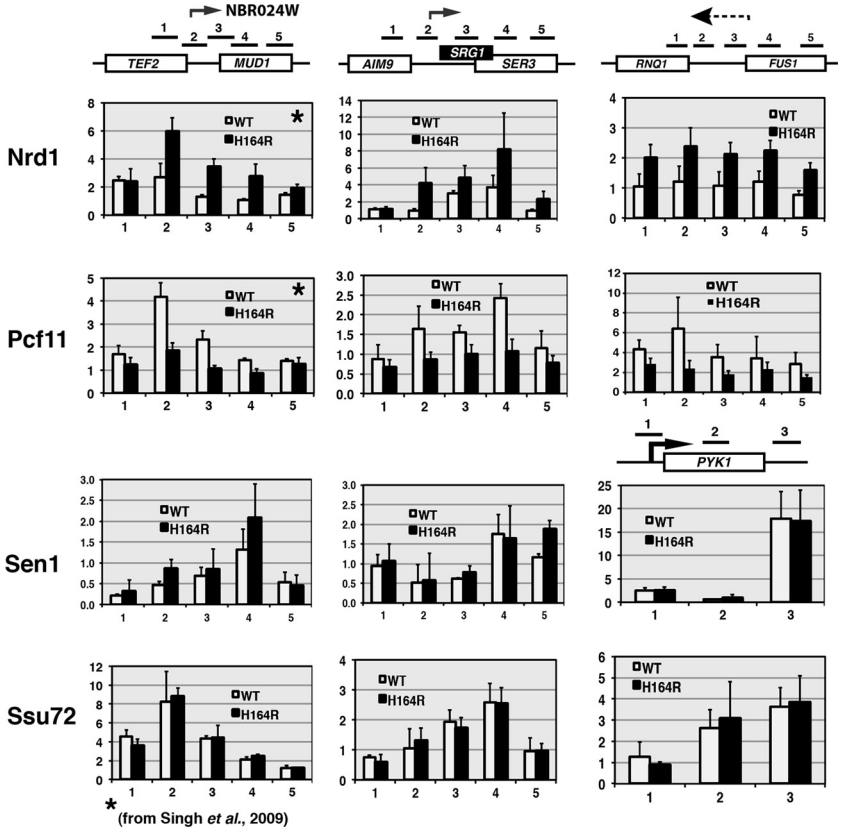

FIG 4 Recruitment of some (Nrd1 and Pcf11) but not other termination factors (Sen1 and Ssu72) is altered in *ess1* mutants. ChIP analysis of four termination factors was performed. No significant effects were detected on recruitment of termination factors (Sen1 and Ssu72) to the intergenic region of *TEF2-MUD1* or to the *SRG1* ncRNA gene or the *PYK1* control gene. An increase in Nrd1 and a decrease in Pcf11 are observed at the 3′ regions of *TEF2*, *SRG1*, and *RNQ1*, similar to previous results for snoRNA loci (51). The inability to bind or release these factors in *ess1* mutants may contribute to defective termination of these genes. Data in panels indicated by stars are reprinted from Molecular Cell (51) with permission of the publisher and are reproduced here for completeness.

sample was also normalized to an internal control gene (*SNR6*, a pol III product) to control for RNA integrity and real-time amplification efficiency, and the data are the averages of three biological replicates. This approach was very sensitive and detected intergenic transcription in *ess1* mutants even when NMD was operational. However, when NMD was inactivated, the levels of intragenic/readthrough transcription detected in *ess1* mutants increased dramatically (Table 2).

Of the genes analyzed, almost half (6 or 7 of 14) had transcript profiles indicative of readthrough transcription (e.g., *HMG2*, *TAE1*, *TEF2*, *KTR3*, *RNQ1*, *AIM5*, and *YLR173W*), suggesting that Ess1 is required for efficient termination of a substantial number of mRNA genes. These results cannot be the result of overall changes in the expression of these genes in the mutant strains, as this was accounted for by the normalization to upstream products. Interestingly, in *ESS1*$^{+}$ cells in which NMD is inactivated, some readthrough is also detected (e.g., *TAE1* and *KTR3*), indicating that a basal level of readthrough occurs even in wild-type cells but these transcripts are normally degraded. CUTs were also prevalent in *ess1* backgrounds (8 of 14 loci). Some occurred at loci that were also exhibiting hallmarks of mRNA readthrough (3 of 8). CUTs also fell into two groups, those that are stabilized in the NMD-deficient background (e.g., *YPR114W-RGC1*) and those that are not (e.g., *SLM1-SHQ1*). The data indicate that some CUTs are subject to degradation by NMD. For both qualitative and quantitative experiments, controls in which no reverse transcriptase was added to the RNA samples ruled out potential DNA contamination (Fig. 7B and data not shown).

To confirm the qRT-PCR results and to investigate the nature of the readthrough products, we carried out Northern analysis on a subset of the above-mentioned genes. Consistent with the qRT-PCR results, we detected aberrantly long transcripts in *ess1*^{ts} mutants whose abundance increased in the NMD mutant background (*ess1*^{ts} *upf1*) (Fig. 7C). These transcripts were more prominent at the restrictive temperature (37°C) (Fig. 7C and D) than at 30°C (data not shown), as expected. To confirm that the longer transcripts were indeed readthrough products (i.e., fusion transcripts), duplicate blots were probed with the downstream genes (*RGD1* and *FTH1*) (Fig. 7C). The same aberrant products were detected using the downstream probes, and their sizes were consistent with termination occurring after the downstream gene. Longer exposures of these gels revealed upward smears of signal from the readthrough bands, suggesting the presence of additional readthrough transcripts with a range of extended 3′ ends (data not shown). Readthrough transcripts were also observed for three additional loci that were examined (Fig. 7D).

Finally, to ensure that transcription readthrough was not simply a consequence of slow growth at 30°C of the *ess1 upf1* double mutants, we also analyzed six other slow-growing strains, obtained from the C. Boone *ts* collection (University of Toronto), by

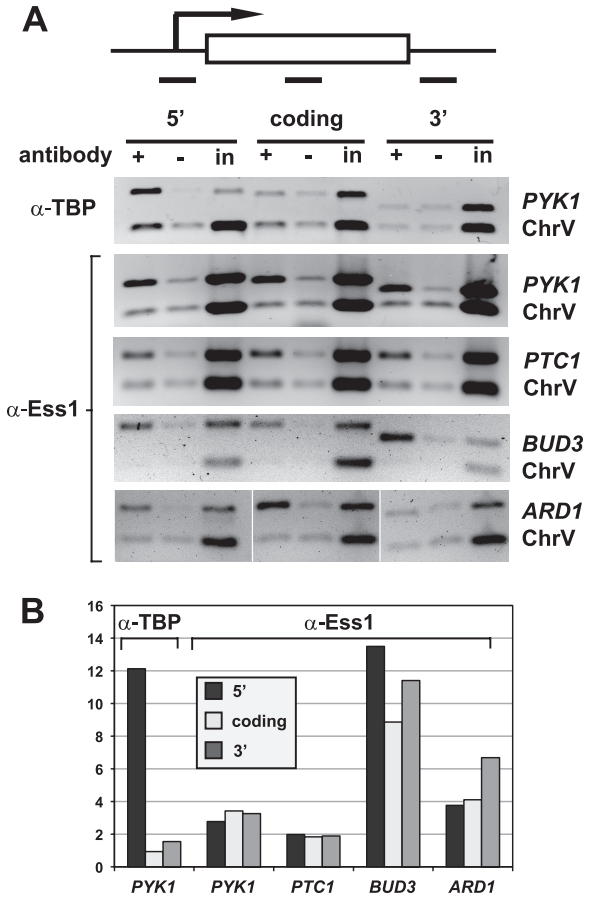

FIG 5 Ess1 is present along transcribed protein-coding genes of all sizes. (A) Results of ChIP with antibodies to Ess1 to monitor the presence of Ess1 at 5′, coding, and 3′ regions of four protein-coding genes. No-antibody and input chromatin (in) controls are included. Shown are representative ethidium bromide-stained gels (image inverted) of PCR products for *PYK1*, *PTC1*, *BUD3*, and *ARD1* genes, as well as an untranscribed region of chromosome V (ChrV). Results of a ChIP for TBP are also included. (B) Quantitation of the results in panel A, with ChIP signals normalized to input and ChrV signals [(IP/input)/(IP/input$_{ChrV}$)]. Similar results were obtained when ChIP signals were normalized to those of no-antibody controls (not shown).

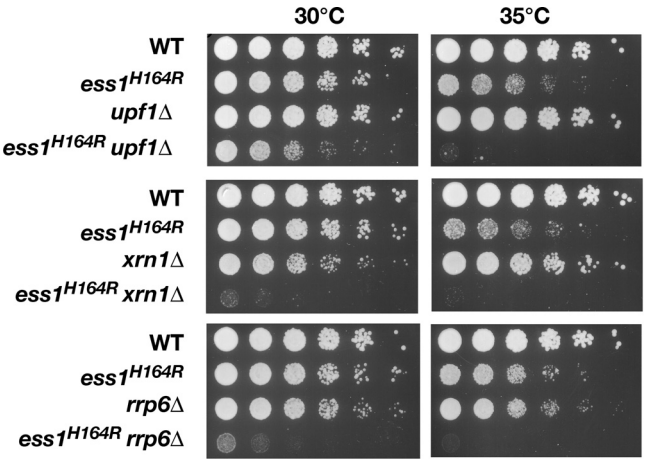

FIG 6 Ess1 mutants are synthetic lethal with NMD and RNA decay mutants. Serial dilutions (1:5, starting with cells at an OD_{600} of 0.5) of the wild type or the indicated mutant cells were grown at 30°C or 35°C on YEPD for 3 days. At both permissive (30°C) and semipermissive (35°C) temperatures, the growth defect of the *ess1*^{H164R} mutant is strongly enhanced by *upf1* (NMD pathway), *xrn1* (cytoplasmic nuclease), and *rrp6* (nuclear exonuclease) mutations. At 35°C, growth of the double mutants was negligible. Single *upf1* mutants have no discernible growth defects, while *xrn1* and *rrp6* mutants have only minor growth defects at 30°C or 35°C, respectively.

qRT-PCR. Five of the six mutants showed no evidence of readthrough defects on seven different loci examined (data not shown). Mutations in these strains (*lcb1-1*, *kar2-159*, *hts1-1*, *pri2-1*, and *bos1-1* mutants) are unrelated to transcription or mRNA processing. The sixth mutant (*srm1-ts*) did show increased intergenic transcription relative to the amount in the wild type. However, this was not entirely surprising given that *SRM1*, also known as *PRP20* (for pre-mRNA processing), is required for mRNA biogenesis and nucleocytoplasmic trafficking and, like *ESS1*, interacts genetically with the NMD pathway (*UPF2*) (13).

On the basis of these results, we suggest that Ess1 is required for efficient termination of the transcription of a sizable fraction (perhaps half) of mRNA genes *in vivo* and that the bulk of aberrant transcripts produced in *ess1* mutants are degraded by NMD. Genome-wide double-mutant analysis would give us a better indication of the total number of genes whose transcription termination is Ess1 dependent.

Ess1 promotes H3K4 trimethylation. The results described above show that Ess1 targets the phosphorylated Ser5-CTD form of RNA pol II *in vivo*. pSer5-CTD levels are highest near the 5′ ends of active genes, and a number of components of the histone modification machinery seem to require pSer5-CTD for binding (18, 42). We therefore asked whether Ess1 might play a role in histone modification, for example, by altering the conformation of the CTD and/or influencing its phosphorylation state, thereby effecting the recruitment or activity of histone-modifying enzymes. We first took a genetic approach, using mutants with mutations of the Set1 and Set2 histone methyltransferases. Set1, as part of the COMPASS complex, generates a trimethylation mark, H3K4me3, which is associated with the 5′ ends of active genes (reviewed in reference 50). Importantly, this mark has been also associated with Nrd1-dependent termination (55). Set2 trimethylates H3K36, and the modified histone helps recruit the Rpd3S deacetylase complex in the wake of elongating polymerase to help reform repressive chromatin to prevent cryptic transcription (10, 25).

We found that *ess1*^{H164R} *set1*Δ double mutants showed synthetic slow growth/lethality, while high-copy-number expression of Set1 rescued the growth defect of *ess1*^{H164R} cells at 37°C (Fig. 8). These results lead to the inference that Ess1 positively affects H3K4 methylation. If true, then in *ess1* mutant cells, H3K4 methylation would decrease, leading to slow growth, and this growth defect should be reversed by mutation of the H3K4 demethylase, Jhd2. Indeed, *jhd2*Δ partially suppressed the *ess1* growth defect at 37°C (Fig. 8). In contrast, the *ess1*^{H164R} *set2*Δ double mutants showed genetic suppression whereby *set2*Δ rescued the growth defect of *ess1* mutants (Fig. 8, bottom).

To determine whether Ess1 affects H3K4 methylation, we used Western analysis to compare the bulk H3K4me3 levels in wild-type and *ess1* mutant cells (Fig. 9A). In *ess1*^{H164R} and *ess1*Δ *srb10*Δ mutants, H3K4me3 levels were reduced relative to the levels in their respective control strains (the wild type and *srb10*Δ). No change occurred in the overall levels of either H3K36me3 or H3

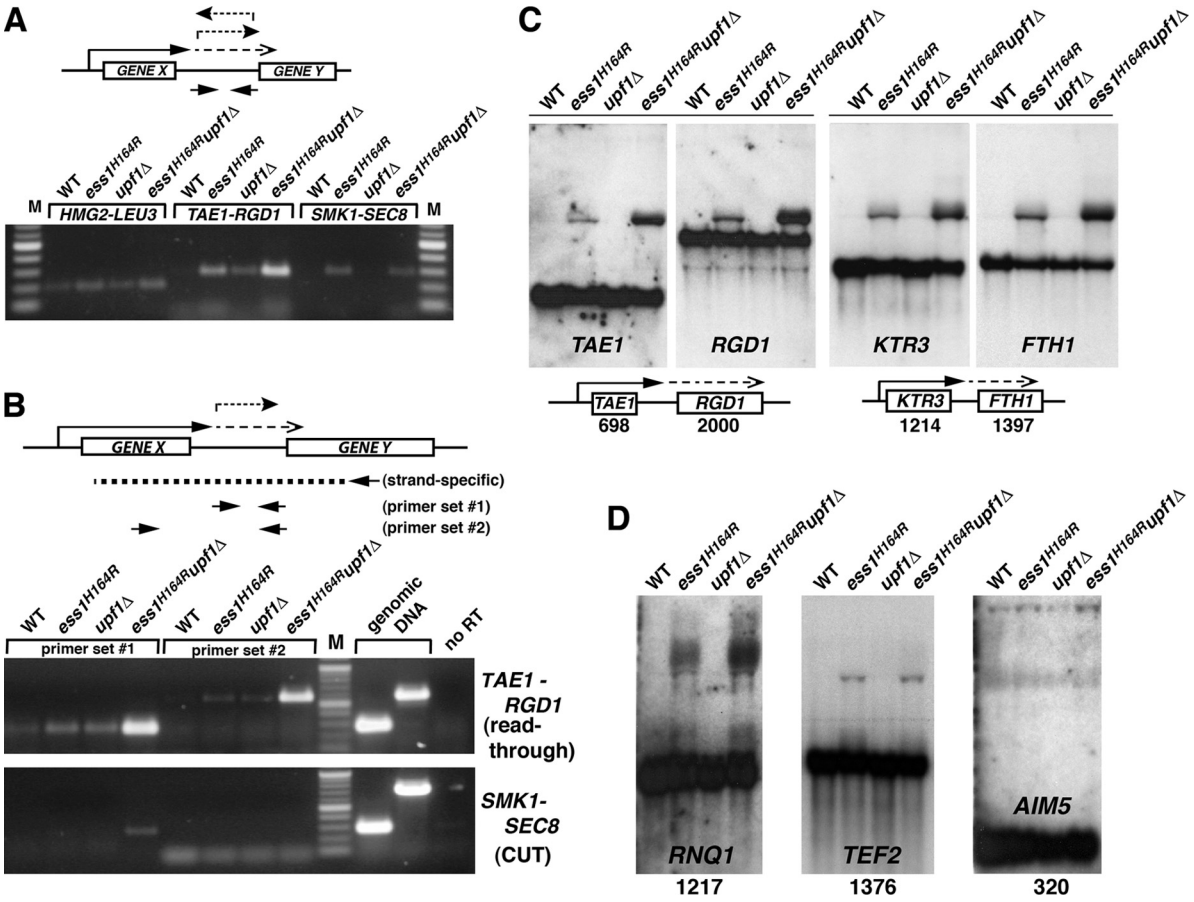

FIG 7 Strong mRNA termination defects were detected in *ess1* mutants using cells that lack nonsense-mediated decay. (A) Intergenic transcription is detected in *ess1* mutants. Quantitative reverse transcription–RT-PCR was used to detect intergenic transcription. Results are shown for three representative loci, *HMG2-LEU3*, *TAE1-RGD1*, and *SMK1-SEC8*. Total RNA from the indicated strains was reverse transcribed using random hexamer primers, and the cDNA products were amplified by PCR for 30, 30, and 34 cycles, respectively, and visualized on an agarose gel. Intergenic primers were used for PCR as indicated in the schematic. (B) Ess1 mutants fail to terminate at mRNA genes, and the readthrough transcripts are degraded by NMD. In contrast to the experiment whose results are shown in panel A, gene-specific primers were used for first-strand cDNA synthesis (see schematic) to allow strand-specific detection of intergenic transcripts (primer set 1), as well as the longer fusion transcripts (primer set 2). The presence of long products at the *TAE1-RGD1* locus in *ess1*^{H164R} mutant cells indicates mRNA readthrough. Thirty cycles were used for PCR. Genomic DNA controls show the efficacy of the primers. Mixtures for control reactions without reverse transcription (no RT) contained 4× as much input template as the experimental samples. (C) Northern analysis of *ess1* and *ess1 upf1* double mutants and controls showing aberrantly long (readthrough) transcripts. Fifteen micrograms of total RNA was used. The ^{32}P-labeled probes (specific activity, $>5 \times 10^8$/μg DNA) were generated from the open reading frames of the genes indicated. The numbers refer to the sizes of the open reading frames in base pairs. Both the upstream and downstream gene probes at each locus were used. (D) Additional loci are analyzed as described for panel C, except that only the upstream gene probe for each locus was used. Ten micrograms of total RNA was used for these samples.

and tubulin in the controls. We also monitored H3K4me3 and H3K36me3 levels across individual genes using ChIP and found significant reductions in H3K4me3 in *ess1* mutants on two out of three loci examined (*TEF2-MUD1* and *SRG1-SER3* but not *PYK1*), suggesting that Ess1 promotes H3K4 trimethylation (Fig. 9B). No changes were observed for H3K36me3. Together, the genetic and molecular analyses indicate that Ess1 plays a role in histone modification and that it affects some modifications more than others.

DISCUSSION

Covalent and noncovalent modifications of the CTD. In this work, we monitored the impact of Ess1 mutations on transcription, CTD phosphorylation, and the recruitment of cofactors to transcribed genes. Although the isomerization state of the CTD cannot be measured directly *in vivo*, we detected widespread transcription defects in cells in which the catalytic activity of the Ess1 enzyme is compromised. The most commonly used allele, *ess1*^{H164R}, which is temperature sensitive for growth, has less than 0.01% of the activity of the wild type on phospho-CTD peptides *in vitro* (17) and is likely to cause substantial alterations in CTD structure and function *in vivo*. Consistent with a role for Ess1 in regulating RNA pol II activity, we could immunoprecipitate pol II (mostly the pSer5 form) with Ess1 (Fig. 1), and using ChIP, we showed that Ess1 is recruited to the 5′, middle, and 3′ regions of the protein-coding genes examined (Fig. 5).

Ess1 is required to keep CUTs silent. A previous tiling array study showed a dramatic increase in the number of CUTs in *ess1* mutants, due in part to faulty transcription termination (and stabilization) of small ncRNAs (51). In this work, ChIP analysis of *ess1* mutants at selected CUT/SUT loci (Fig. 2 and 3) showed increased recruitment of the Ser5-phosphorylated form of RNA pol

TABLE 2 Results of quantitative reverse transcription–real-time PCR across selected intergenic regions

Locus	cDNA primer[a]	Primer set	Normalized ΔC_T value ± SD[b]			Interpretation
			ess1^{H164R}	*upf1*Δ	*ess1*^{H164R} *upf1*Δ	
PTP1-SSB1	RH	1	0.34 ± 0.56	2.45 ± 5.82	0.58 ± 0.88	No aberrant transcripts
GUS1-RTF1	RH	1	0.40 ± 0.99	6.59 ± 3.93	3.68 ± 1.24	
TAE1-RGD1	RH	1	11.79 ± 1.05	9.85 ± 0.39	68.95 ± 1.02	Readthrough
	GSS	1	6.37 ± 0.75	3.74 ± 1.12	226.76 ± 0.66	
	GSS	2	24.20 ± 1.18	12.01 ± 1.56	1,166.80 ± 0.51	
SMK1-SEC8	RH	1	18.77 ± 1.03	4.54 ± 1.30	28.80 ± 1.03	CUT
	GSS	1	2.36 ± 0.38	ND	9.63 ± 0.39	
	GSS	2	ND	ND	ND	
KTR3-FTH1	RH	1	27.54 ± 0.54	8.37 ± 1.63	58.42 ± 0.55	CUT (reverse) and readthrough
	GSS	1	3.63 ± 0.76	6.61 ± 1.89	42.23 ± 0.89	
	GSS	2	2.64 ± 0.79	4.75 ± 1.65	24.30 ± 0.77	
RNQ1-FUS1	RH	1	92.41 ± 1.10	10.57 ± 2.79	192.45 ± 0.66	CUT (reverse) and readthrough
	GSS	1	9.49 ± 0.60	5.19 ± 1.73	191.00 ± 0.69	
	GSS	2	77.35 ± 0.53	18.16 ± 1.30	1,103.86 ± 0.34	
TEF2-MUD1	RH	1	594.97 ± 1.08	3.69 ± 1.42	7,152.18 ± 4.05	CUT (forward) and readthrough
	GSS	1	168.90 ± 0.93	5.17 ± 1.46	5,887.07 ± 1.18	
	GSS	2	435.54 ± 1.51	9.17 ± 1.66	9,079.10 ± 1.57	
AIM5-TAE1	RH	1	1.23 ± 1.42	2.59 ± 2.26	3.44 ± 0.95	Readthrough
	GSS	1	0.37 ± 1.18	1.84 ± 4.36	12.29 ± 2.20	
	GSS	2	1.50 ± 0.97	6.53 ± 4.88	55.66 ± 2.07	
YPR114W-RGC1	RH	1	91.35 ± 0.33	4.07 ± 0.77	12,677.66 ± 1.31	CUT (reverse)
	GSS	1	1.27 ± 0.56	2.19 ± 4.13	9.84 ± 0.84	
	GSS	2	1.05 ± 0.92	1.57 ± 6.66	1.26 ± 0.42	
HMG2-LEU3	RH	1	3.47 ± 0.41	5.68 ± 2.22	15.21 ± 1.20	Possible (minor) readthrough
	GSS	1	0.84 ± 0.49	0.92 ± 0.67	3.18 ± 1.25	
	GSS	2	0.33 ± 0.49	1.85 ± 1.01	11.24 ± 0.14	
FIG4-PFA3	RH	1	1.84 ± 1.72	2.65 ± 1.13	9.18 ± 2.60	CUT (forward)
	GSS	1	255.41 ± 0.80	142.35 ± 1.44	5,395.35 ± 0.94	
	GSS	2	ND	ND	ND	
SLM1-SHQ1	RH	1	34.86 ± 1.02	2.90 ± 4.49	66.48 ± 1.13	CUT (forward)
	GSS	1	17.63 ± 1.34	3.25 ± 4.90	218.40 ± 1.58	
	GSS	2	ND	ND	ND	
YLR173W-IDP2	RH	1	1.69 ± 0.38	4.17 ± 3.13	5.00 ± 0.77	Readthrough
	GSS	1	0.75 ± 0.58	3.39 ± 4.08	10.60 ± 0.96	
	GSS	2	1.85 ± 0.16	25.05 ± 3.96	105.85 ± 0.37	
SKM1-MSB4	RH	1	1.11 ± 1.02	21.61 ± 5.69	13.67 ± 0.52	CUT (forward) revealed by *upf1*Δ
	GSS	1	0.81 ± 1.02	29.45 ± 3.36	13.79 ± 0.78	
	GSS	2	ND	ND	ND	

[a] RH, random hexamers; GSS, gene and strand specific.

[b] All data are expressed as the ratio over the data for the wild type. Data have been normalized to *SNR6* expression (to control for RNA and cDNA integrity and qRT-PCR efficiency) and to a region within the 5′ coding region of the upstream gene (to control for any potential changes in mRNA levels in the mutant backgrounds). See Materials and Methods for details. Primer set locations are approximately as depicted in Fig. 7. cDNA synthesis was primed using either random hexamers or gene-specific primers oriented so as to template only forward transcripts, as indicated. Random-hexamer-primed cDNAs typically resulted in stronger signals than cDNA made using a single gene-specific primer (i.e., using the same PCR primer sets). N.B., for the *FIG4-PFA3* GSS primer set 1 samples, since WT readthrough was undetectable, we set the ΔC_T(control) value to 37 cycles, which is average for samples with no readthrough. ND, none detected.

II, as well as initiation factors TBP and TFIIB and the 5′-capping enzyme Ceg1. This result suggests that, in addition to being required for CUT termination, Ess1 represses the initiation of CUTs and, similarly, keeps SUTs from being overexpressed. The mechanism is not yet clear, but it could be due to direct effects of Ess1 on CTD structure that affect the binding of initiation factors or to indirect effects through changes in CTD phosphorylation or chromatin structure (see below).

A role for Ess1 in initiation was previously suggested by Krishnamurthy et al. (27), based on its strong genetic interaction with

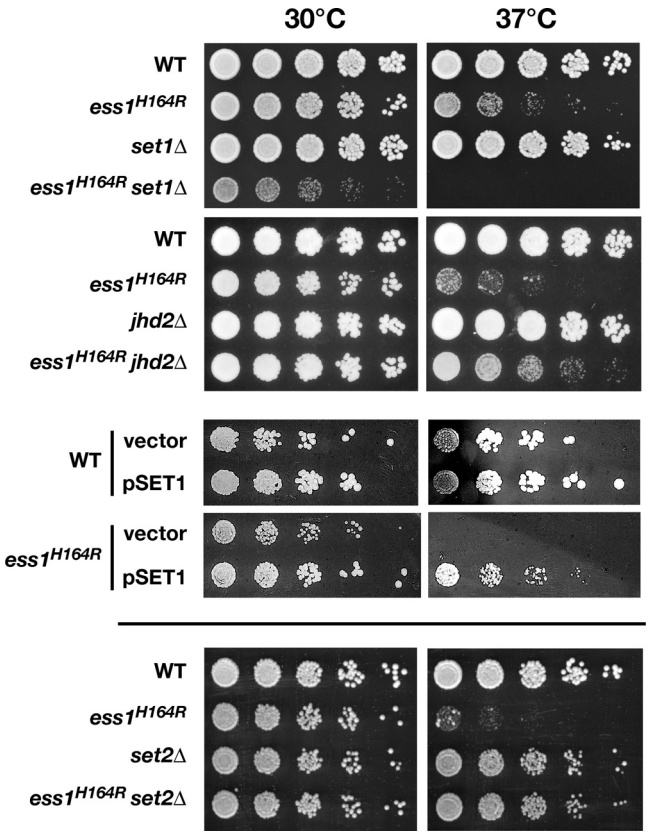

FIG 8 Genetic interactions between *ESS1* and *SET1/JHD2* suggest that Ess1 is required for histone H3K4 methylation. Serial dilutions (1:5) starting at a 1:5 dilution (except for *set1* mutant cells shown in the top panels, which started at 1:1) of wild-type or mutant cells at an OD_{600} of 0.5 were grown at 30°C or 37°C on YEPD for 2 to 3 days or, for the experiments using a plasmid overexpressing *SET1* (pSET1), on CSM minus uracil (49) for 4 days. Deletion of the gene encoding the Set1 histone methyltransferase is synthetic lethal with $ess1^{H164R}$, whereas deletion of *JHD2*, the gene encoding the H3K4 demethylase, rescues $ess1^{H164R}$ cells. The plasmid that overexpresses *SET1* (pMP803-ADH/SET1) suppresses the growth defects of $ess1^{H164R}$ cells at permissive (30°C) and nonpermissive (37°C) temperatures, but the control vector (pRS416) does not. A *set2*Δ mutant rescues growth of $ess1^{H164}$ cells at 37°C.

SUA7, which encodes TFIIB. These authors found *ess1* mutants to be defective for the induction of *GAL1*, *PHO5*, and *INO1* reporters (although they did not formally demonstrate that this was due to initiation defects). We found no effect of Ess1 on the recruitment of initiation factors to a control mRNA gene, *PYK1*. One difference is that *PYK1* is constitutively expressed, whereas the genes studied by Krishnamurthy et al. are highly inducible. Thus, the function of Ess1 during initiation may vary depending on the mRNA gene, probably because of the requirements for different combinations of regulators at individual promoters.

Ess1 is important for mRNA termination. Early studies recovered Ess1 (Ptf1) in a genetic screen for defective 3′-end processing/termination (21, 22). Later work showed readthrough of reporter constructs in *ess1* mutant cells (27, 64). However, none of these studies clearly demonstrated readthrough of chromosomal genes. Even genome-wide tiling array analysis revealed only a small number of mRNAs exhibiting readthrough in *ess1* mutants (51). Perhaps the nuclear and/or cytoplasmic RNA quality control mechanisms (reviewed in references 16 and 39) were degrading the readthrough transcripts in *ess1* mutants, explaining why they eluded detection. Indeed, inactivating NMD, the major RNA surveillance system, revealed strong readthrough in *ess1* mutants in almost half of the chromosomal mRNA genes tested (Fig. 7 and Table 2). Although the results were complicated by the induction and stabilization of intergenic CUTs (in *ess1* mutants), we could distinguish these from transcription readthrough and showed that Ess1 is required for efficient mRNA termination in yeast. It is likely that some mRNA readthrough products are subject to degradation by pathways other than NMD (e.g., Rrp6/nuclear exosome), and thus, our estimate of about half of mRNA genes being dependent on Ess1 for efficient termination might be an underestimate.

While we do not know how readthrough transcripts in *ess1* mutants reach the cytoplasm, the site of NMD-mediated RNA decay, there are several possibilities. Termination and polyadenylation may occur in the downstream gene at cryptic or normal poly(A) sites. In this case, the transcripts would be exported from the nucleus and would trigger NMD due to premature termination codons encoded in the intergenic regions. Indeed, our Northern analysis, which detected discrete-length readthrough transcripts, was consistent with this idea. Second, it is possible that in *ess1* mutants, the normal RNA quality control mechanisms for export are defective or are saturated by widespread mRNA readthrough products, thereby allowing the defective transcripts to enter the cytoplasm for degradation. There was also evidence for transcripts with heterogeneous 3′ ends in *ess1 upf1* double mutants, as detected by Northern analysis. It is possible that these are incorrectly processed mRNAs.

The defect in mRNA termination in *ess1* mutants is probably due to a failure to coordinate the recruitment and release of key termination factors. Pcf11 recruitment to the 3′ end of several genes was reduced in *ess1* mutants (Fig. 4), while the levels of Nrd1, which is not known to function in mRNA termination, increased, perhaps inhibiting the process. Both proteins are sensitive to the phosphorylation state of the CTD, with Nrd1 preferring the pSer5 form and Pcf11 preferring the pSer2 form (59). Ess1's effect on their recruitment may therefore be due to changes in CTD phosphorylation, with *ess1* mutants showing increased levels of pSer5 (27, 51) and pSer7 (Fig. 1). Bataille et al. showed by genome-wide ChIP with microarray technology (ChIP-chip) analysis that both pSer5 and pSer7 levels increased significantly at the 3′ ends of nearly all protein-coding genes in *ess1* mutants (6). Interestingly, pSer7 in human cells is important for the recruitment of the RPAP2 Ser5-specific phosphatase (Rtr1 in yeast) to small nuclear RNA genes, also suggesting a functional linkage between these two marks that may also be critical for termination, although a distinct mechanism seems to operate at mRNA genes (15).

Ess1 probably increases the activity of the Ssu72 phosphatase, which prefers the *cis* form of CTD peptide substrates (61) and targets both pSer5 and pSer7 in the CTD (6). We found no significant changes in the levels of Ssu72 at several loci in *ess1* mutants (Fig. 4 and data not shown), suggesting that Ess1 affects its activity on its substrate(s) but not its recruitment. Many other factors are required for mRNA termination and 3′-end processing in yeast (28), and genetic studies suggest that at least some are influenced by Ess1 (C. Barnes, J. Alafifi, and S. Hanes, unpublished observations).

Ess1 is important for H3K4 methylation. Prompted by close linkages between histone modifiers and the CTD (e.g., see refer-

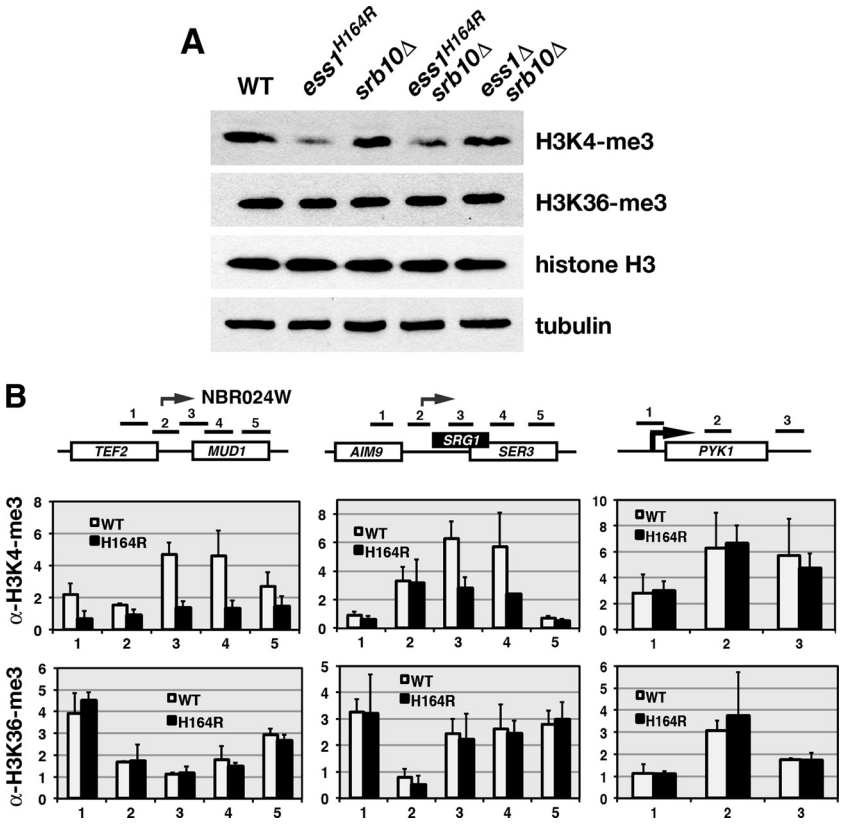

FIG 9 Levels of H3K4me3 are reduced in *ess1* mutants. (A) Western analysis using protein from whole-cell extracts probed with the indicated antibodies (see Materials and Methods for details). Cells were grown at 30°C. Bulk levels of H3K4me3 are reduced in *ess1* mutants. Levels of H3K36 methylation were unchanged, as were overall levels of histone H3. Tubulin was used as a loading control to assess protein integrity and concentration. Equal amounts of protein (10 μg) were loaded in all wells. Blots were generated individually and not reprobed. (B) ChIP analysis to monitor levels of H3K4me3 in *ess1* mutants along individual gene loci *TEF2-MUD1* and *SRG1-SER3*. Levels of H3K4me3 but not H3K36me3 are reduced across ncRNA loci. No effect was observed at *PYK1*. Fold changes are relative to the results for H3 after normalization to a chromosome V control (H3K36me3) or a tRNA gene control (H3K4me3). Error bars show standard deviations of three biological replicates.

ences 18 and 42; reviewed in reference 8) and prior studies linking *ess1* to the *rpd3* histone deacetylase and Gcn5 histone acetyltransferase (4), we investigated the link between Ess1 and two additional histone modifiers, Set1 and Set2. The Set1 H3K4 histone methyltransferase specifically targets the pSer5 form of RNA polymerase and is associated with active transcription (42). The Set2 H3K36 methyltransferase, which contains a WW domain, binds the doubly phosphorylated form (pSer2/pSer5) and is associated with elongating polymerases (30, 44). Our results indicate a functional link between Ess1 and histone H3K4 methylation by Set1 (Fig. 8 and 9). In contrast, although we found strong genetic interactions between *ESS1* and *SET2* (Fig. 8), we did not detect changes in H3K36 trimethylation (Fig. 9).

Ess1 may help recruit Set1 to the early form of elongating polymerase. This may occur directly, by conformation-induced changes in CTD structure, or indirectly, through Ess1's effect on Ser5 CTD phosphorylation or, potentially, on other histone modifications. For example, *ess1* is synthetic lethal with a deletion of *RAD6* (data not shown), which encodes a ubiquitin-conjugating enzyme (E2) that monoubiquitylates histone H2B at lysine 123 (45). H2B K123 ubiquitylation is coupled to H3K4 trimethylation by Set1 (40, 54). If indeed Ess1 is important for Rad6 activity, then loss of Ess1 would indirectly reduce H3K4 methylation. This would be consistent with genetic results that show the opposite genetic relationship between $ess1^{H164R}$ and *set1*Δ (synthetic lethality) versus that of $ess1^{H164R}$ and *set2*Δ (rescue), since Rad6-dependent ubiquitylation of H2B is positively associated with Set1-dependent H3K4 trimethylation but negatively associated with Set2-dependent H3K36 activity (23). Finally, it is possible that Ess1 acts directly on Set1 protein or other subunits of the COMPASS complex to stimulate their activity. Localization of Set1p by ChIP in *ess1* mutants may help distinguish between these models.

Two recent studies are of special interest. First, Wang et al. (60) found that H3K4me3 can prevent promoter activation by recruitment of the Rpd3L deacetylase complex. When H3K4me3 levels are reduced, Rpd3L is not recruited and basal transcription of the *PHO5* promoter is derepressed (i.e., in under high-Pi conditions), probably due to increased H3 and H4 acetylation and a more open chromatin structure. A similar mechanism could occur at CUT loci in *ess1* mutants, which show decreased H3K4me3 levels (Fig. 9) and increased recruitment of pol II and initiation factors (Fig. 2 and 3). Thus, loss of Ess1 function would reduce H3K4me3 and would lower histone deacetylase (Rpd3L) recruitment at cryptic promoters and derepress their transcription.

In the second study, Terzi et al. (55) showed that deletion of *SET1* reduced Nrd1 recruitment, resulting in transcription readthrough of snoRNAs and CUTs. Their results suggested a model in which Set1 H3K4 trimethylation recruits RpdL, as well as the

NuA3 histone acetyltransferase, and that the proper balance of acetylation at these promoters is necessary to load the Nrd1-Nab3-Sen1 termination complex onto the elongating polymerase. We also see readthrough of snoRNAs and CUTs in *ess1* mutants (51), as well as decreased H3K4me3 (Fig. 9). However, we do not see reduced Nrd1 recruitment but, rather, results consistent with a failure of exchange of Nrd1 (increased levels) and Pcf11 (decreased levels) (Fig. 4) (51). Perhaps this indicates that the rate of exchange of termination factors, facilitated by CTD isomerization, is as important as the absolute levels of recruitment. Interestingly, Terzi et al. (55) found no effect of *set1*Δ on mRNA termination, suggesting that the mRNA readthrough defects we detect in *ess1* mutants are probably not mediated through changes in levels of H3K4 trimethylation.

Ess1 function in termination might be conserved. The biochemical activities of Ess1 and Pin1 are similar (72), and the fact that *PIN1* genes from *Drosophila* (34), *Xenopus* (C. B. Wilcox and S. D. Hanes, unpublished), and humans (32) rescue *ess1*Δ mutants indicates a conserved *in vivo* function. Preliminary experiments in human (HeLa) cells suggest that small interfering RNA knockdown of Pin1 may cause readthrough of snoRNAs (A. Burch, Z. Ma, S. Hanes, data not shown). Prior studies showed Pin1-dependent inhibition of transcription *in vitro* (69), and overexpression of Pin1 increased CTD phosphorylation levels on Ser5 (68). This later effect was opposite to that observed in yeast (overexpression of Ess1 decreased pSer5 [51]); however, it nonetheless supports the idea that Ess1 controls RNA pol II function in all eukaryotes. It remains to be determined whether Pin1 is important for mRNA termination. Further studies should provide the answers.

ACKNOWLEDGMENTS

We are grateful to David Brow, Joan Curcio, Steve Buratowski, Brian Dichtl, Dirk Eick, Mike Hampsey, Caroline Kane, Ian Willis, and Anthony Weil for plasmids, strains, or antibodies, to the Wadsworth Center Molecular Genetics and Media facilities, and to Dave Amberg, Randy Morse, Navjot Singh, and Joe Wade for helpful discussions. We thank Taylor Moon (SUNY—Upstate Summer Undergraduate Fellow) for pilot qRT-PCR experiments and April Burch (Wadsworth Center) for Pin1 experiments.

S.D.H. dedicates this paper to the memory of his mother, Helen Hanes, who first introduced him to research at the famed Bell Telephone Laboratories in Murray Hill, NJ.

This work was funded by grants to S.D.H. from the NIH (grants 3R01-GM055108 and ARRA-GM055108-S1), the NSF (grant MCB-0613001), and SUNY—Upstate Medical University.

REFERENCES

1. **Amrani N, et al.** 2006. Aberrant termination triggers nonsense-mediated mRNA decay. Biochem. Soc. Trans. **34**:39–42.
2. **Amrani N, et al.** 1997. PCF11 encodes a third protein component of yeast cleavage and polyadenylation factor I. Mol. Cell. Biol. **17**:1102–1109.
3. **Andrecka J, et al.** 2008. Single-molecule tracking of mRNA exiting from RNA polymerase II. Proc. Natl. Acad. Sci. U. S. A. **105**:135–140.
4. **Arevalo-Rodriguez M, Cardenas ME, Wu X, Hanes SD, Heitman J.** 2000. Cyclophilin A and Ess1 interact with and regulate silencing by the Sin3-Rpd3 histone deacetylase. EMBO J. **19**:3739–3749.
5. **Arevalo-Rodriguez M, Wu X, Hanes SD, Heitman J.** 2004. Prolyl isomerases in yeast. Front. Biosci. **9**:2420–2446.
6. **Bataille AR, et al.** 2012. A universal RNA polymerase II CTD cycle is orchestrated by complex interplays between kinase, phosphatase and isomerase enzymes along genes. Mol. Cell **45**:158–170.
7. **Buratowski S.** 2003. The CTD code. Nat. Struct. Biol. **10**:679–680.
8. **Buratowski S.** 2009. Progression through the RNA polymerase II CTD cycle. Mol. Cell **36**:541–546.
9. **Buratowski S, Kim T.** 2010. The role of cotranscriptional histone methylations. Cold Spring Harb. Symp. Quant. Biol. **75**:95–102.
10. **Carrozza MJ, et al.** 2005. Histone H3 methylation by Set2 directs deacetylation of coding regions by Rpd3S to suppress spurious intragenic transcription. Cell **123**:581–592.
11. **Chapman RD, et al.** 2007. Transcribing RNA polymerase II is phosphorylated at CTD residue serine-7. Science **318**:1780–1782.
12. **Conrad NK, et al.** 2000. A yeast heterogeneous nuclear ribonucleoprotein complex associated with RNA polymerase II. Genetics **154**:557–571.
13. **Costanzo M, et al.** 2010. The genetic landscape of a cell. Science **327**:425–431.
14. **Egloff S, Murphy S.** 2008. Cracking the RNA polymerase II CTD code. Trends Genet. **24**:280–288.
15. **Egloff S, Zaborowska J, Laitem C, Kiss T, Murphy S.** 2012. Ser7 phosphorylation of the CTD recruits the RPAP2 Ser5 phosphatase to snRNA genes. Mol. Cell **45**:111–122.
16. **Fasken MB, Corbett AH.** 2009. Mechanisms of nuclear mRNA quality control. RNA Biol. **6**:237–241.
17. **Gemmill TR, Wu X, Hanes SD.** 2005. Vanishingly low levels of Ess1 prolyl-isomerase activity are sufficient for growth in *Saccharomyces cerevisiae*. J. Biol. Chem. **280**:15510–15517.
18. **Govind CK, et al.** 2010. Phosphorylated Pol II CTD recruits multiple HDACs, including Rpd3C(S), for methylation-dependent deacetylation of ORF nucleosomes. Mol. Cell **39**:234–246.
19. **Halbach A, et al.** 2009. Cotranslational assembly of the yeast *SET1*C histone methyltransferase complex. EMBO J. **28**:2959–2970.
20. **Hanes SD, Shank PR, Bostian KA.** 1989. Sequence and mutational analysis of *ESS1*, a gene essential for growth in *Saccharomyces cerevisiae*. Yeast **5**:55–72.
21. **Hani J, et al.** 1999. Mutations in a peptidylprolyl-cis/trans-isomerase gene lead to a defect in 3′-end formation of a pre-mRNA in *Saccharomyces cerevisiae*. J. Biol. Chem. **274**:108–116.
22. **Hani J, Stumpf G, Domdey H.** 1995. *PTF1* encodes an essential protein in *Saccharomyces cerevisiae*, which shows strong homology with a new putative family of PPIases. FEBS Lett. **365**:198–202.
23. **Henry KW, et al.** 2003. Transcriptional activation via sequential histone H2B ubiquitylation and deubiquitylation, mediated by SAGA-associated Ubp8. Genes Dev. **17**:2648–2663.
24. **Hirose Y, Ohkuma Y.** 2007. Phosphorylation of the C-terminal domain of RNA polymerase II plays central roles in the integrated events of eucaryotic gene expression. J. Biochem. **141**:601–608.
25. **Keogh MC, et al.** 2005. Cotranscriptional set2 methylation of histone H3 lysine 36 recruits a repressive Rpd3 complex. Cell **123**:593–605.
26. **Kim H, et al.** 2010. Gene-specific RNA polymerase II phosphorylation and the CTD code. Nat. Struct. Mol. Biol. **17**:1279–1286.
27. **Krishnamurthy S, Ghazy MA, Moore C, Hampsey M.** 2009. Functional interaction of the Ess1 prolyl isomerase with components of the RNA polymerase II initiation and termination machineries. Mol. Cell. Biol. **29**:2925–2934.
28. **Kuehner JN, Pearson EL, Moore C.** 2011. Unravelling the means to an end: RNA polymerase II transcription termination. Nat. Rev. Mol. Cell. Biol. **12**:283–294.
29. **Leeds P, Peltz SW, Jacobson A, Culbertson MR.** 1991. The product of the yeast *UPF1* gene is required for rapid turnover of mRNAs containing a premature translational termination codon. Genes Dev. **5**:2303–2314.
30. **Li J, Moazed D, Gygi SP.** 2002. Association of the histone methyltransferase Set2 with RNA polymerase II plays a role in transcription elongation. J. Biol. Chem. **277**:49383–49388.
31. **Li Z, et al.** 2011. Systematic exploration of essential yeast gene function with temperature-sensitive mutants. Nat. Biotechnol. **29**:361–367.
32. **Lu KP, Hanes SD, Hunter T.** 1996. A human peptidyl-prolyl isomerase essential for regulation of mitosis. Nature **380**:544–547.
33. **Lu KP, Zhou XZ.** 2007. The prolyl isomerase PIN1: a pivotal new twist in phosphorylation signalling and disease. Nat. Rev. Mol. Cell Biol. **8**:904–916.
34. **Maleszka R, Hanes SD, Hackett RL, de Couet HG, Miklos GL.** 1996. The *Drosophila melanogaster dodo* (*dod*) gene, conserved in humans, is functionally interchangeable with the *ESS1* cell division gene of *Saccharomyces cerevisiae*. Proc. Natl. Acad. Sci. U. S. A. **93**:447–451.
35. **Martens JA, Wu PY, Winston F.** 2005. Regulation of an intergenic transcript controls adjacent gene transcription in *Saccharomyces cerevisiae*. Genes Dev. **19**:2695–2704.

36. **Mayer A, et al.** 2010. Uniform transitions of the general RNA polymerase II transcription complex. Nat. Struct. Mol. Biol. **17**:1272–1278.
37. **Meinhart A, Kamenski T, Hoeppner S, Baumli S, Cramer P.** 2005. A structural perspective of CTD function. Genes Dev. **19**:1401–1415.
38. **Morris DP, Phatnani HP, Greenleaf AL.** 1999. Phospho-carboxyl-terminal domain binding and the role of a prolyl isomerase in pre-mRNA 3′-end formation. J. Biol. Chem. **274**:31583–31587.
39. **Muhlemann O, Eberle AB, Stalder L, Zamudio Orozco R.** 2008. Recognition and elimination of nonsense mRNA. Biochim. Biophys. Acta **1779**:538–549.
40. **Nakanishi S, et al.** 2009. Histone H2BK123 monoubiquitination is the critical determinant for H3K4 and H3K79 trimethylation by COMPASS and Dot1. J. Cell Biol. **186**:371–377.
41. **Neil H, et al.** 2009. Widespread bidirectional promoters are the major source of cryptic transcripts in yeast. Nature **457**:1038–1042.
42. **Ng HH, Robert F, Young RA, Struhl K.** 2003. Targeted recruitment of Set1 histone methylase by elongating Pol II provides a localized mark and memory of recent transcriptional activity. Mol. Cell **11**:709–719.
43. **Phatnani HP, Greenleaf AL.** 2006. Phosphorylation and functions of the RNA polymerase II CTD. Genes Dev. **20**:2922–2936.
44. **Phatnani HP, Jones JC, Greenleaf AL.** 2004. Expanding the functional repertoire of CTD kinase I and RNA polymerase II: novel phosphoCTD-associating proteins in the yeast proteome. Biochemistry **43**:15702–15719.
45. **Robzyk K, Recht J, Osley MA.** 2000. Rad6-dependent ubiquitination of histone H2B in yeast. Science **287**:501–504.
46. **Schiene C, Fischer G.** 2000. Enzymes that catalyse the restructuring of proteins. Curr. Opin. Struct. Biol. **10**:40–45.
47. **Schiene-Fischer C, Aumuller T, Fischer G. 20 May**2011. Peptide bond cis/trans isomerases: a biocatalysis perspective of conformational dynamics in proteins. Top. Curr. Chem. [Epub ahead of print.] doi:10.1007/128_2011_151.
48. **Schmitt ME, Brown TA, Trumpower BL.** 1990. A rapid and simple method for preparation of RNA from *Saccharomyces cerevisiae*. Nucleic Acids Res. **18**:3091–3092.
49. **Sherman F.** 1991. Getting started with yeast. Methods Enzymol. **194**:3–21.
50. **Shilatifard A.** 2008. Molecular implementation and physiological roles for histone H3 lysine 4 (H3K4) methylation. Curr. Opin. Cell Biol. **20**:341–348.
51. **Singh N, et al.** 2009. The Ess1 prolyl isomerase is required for transcription termination of small non-coding regulatory RNAs via the Nrd1 pathway. Mol. Cell **36**:255–266.
52. **Spain MM, Govind CK.** 2011. A role for phosphorylated Pol II CTD in modulating transcription coupled histone dynamics. Transcription **2**:78–81.
53. **Steinmetz EJ, Brow DA.** 1996. Repression of gene expression by an exogenous sequence element acting in concert with a heterogeneous nuclear ribonucleoprotein-like protein, Nrd1, and the putative helicase Sen1. Mol. Cell. Biol. **16**:6993–7003.
54. **Sun ZW, Allis CD.** 2002. Ubiquitination of histone H2B regulates H3 methylation and gene silencing in yeast. Nature **418**:104–108.
55. **Terzi N, Churchman LS, Vasiljeva L, Weissman J, Buratowski S.** 2011. H3K4 trimethylation by Set1 promotes efficient termination by the Nrd1-Nab3-Sen1 pathway. Mol. Cell. Biol. **31**:3569–3583.
56. **Theuerkorn M, Fischer G, Schiene-Fischer C.** 2011. Prolyl cis/trans isomerase signalling pathways in cancer. Curr. Opin. Pharmacol. **11**:281–287.
57. **Thomas BJ, Rothstein R.** 1989. Elevated recombination rates in transcriptionally active DNA. Cell **56**:619–630.
58. **Tietjen JR, et al.** 2010. Chemical-genomic dissection of the CTD code. Nat. Struct. Mol. Biol. **17**:1154–1161.
59. **Vasiljeva L, Kim M, Mutschler H, Buratowski S, Meinhart A.** 2008. The Nrd1-Nab3-Sen1 termination complex interacts with the Ser5-phosphorylated RNA polymerase II C-terminal domain. Nat. Struct. Mol. Biol. **15**:795–804.
60. **Wang SS, Zhou BO, Zhou JQ.** 2011. Histone H3 lysine 4 hypermethylation prevents aberrant nucleosome remodeling at the PHO5 promoter. Mol. Cell. Biol. **31**:3171–3181.
61. **Werner-Allen JW, et al.** 2011. cis-Proline-mediated Ser(P)5 dephosphorylation by the RNA polymerase II C-terminal domain phosphatase Ssu72. J. Biol. Chem. **286**:5717–5726.
62. **West ML, Corden JL.** 1995. Construction and analysis of yeast RNA polymerase II CTD deletion and substitution mutations. Genetics **140**:1223–1233.
63. **Wilcox CB, Rossettini A, Hanes SD.** 2004. Genetic interactions with C-terminal domain (CTD) kinases and the CTD of RNA Pol II suggest a role for *ESS1* in transcription initiation and elongation in *Saccharomyces cerevisiae*. Genetics **167**:93–105.
64. **Wu X, Rossettini A, Hanes SD.** 2003. The *ESS1* prolyl isomerase and its suppressor *BYE1* interact with RNA pol II to inhibit transcription elongation in *Saccharomyces cerevisiae*. Genetics **165**:1687–1702.
65. **Wu X, et al.** 2000. The Ess1 prolyl isomerase is linked to chromatin remodeling complexes and the general transcription machinery. EMBO J. **19**:3727–3738.
66. **Wyers F, et al.** 2005. Cryptic pol II transcripts are degraded by a nuclear quality control pathway involving a new poly(A) polymerase. Cell **121**:725–737.
67. **Xiang K, et al.** 2010. Crystal structure of the human symplekin-Ssu72-CTD phosphopeptide complex. Nature **467**:729–733.
68. **Xu YX, Hirose Y, Zhou XZ, Lu KP, Manley JL.** 2003. Pin1 modulates the structure and function of human RNA polymerase II. Genes Dev. **17**:2765–2776.
69. **Xu YX, Manley JL.** 2007. Pin1 modulates RNA polymerase II activity during the transcription cycle. Genes Dev. **21**:2950–2962.
70. **Yeh ES, Means AR.** 2007. PIN1, the cell cycle and cancer. Nat. Rev. Cancer **7**:381–388.
71. **Yu C, Palumbo MJ, Lawrence CE, Morse RH.** 2006. Contribution of the histone H3 and H4 amino termini to Gcn4p- and Gcn5p-mediated transcription in yeast. J. Biol. Chem. **281**:9755–9764.
72. **Zhang Y, Fussel S, Reimer U, Schutkowski M, Fischer G.** 2002. Substrate-based design of reversible Pin1 inhibitors. Biochemistry **41**:11868–11877.